Aqueous Solutions next to Phospholipid Membrane Surfaces: Insights from Simulations

Max L. Berkowitz,* David L. Bostick,† and Sagar Pandit‡

Department of Chemistry, University of North Carolina at Chapel Hill, Chapel Hill, North Carolina 27599

Received May 20, 2005

Contents

1. Introduction

It is well established that water plays a very important role in the functioning of biological molecules and their assemblies. Among such molecular assemblies are biological membranes. The self-assembly of these membranes is driven by the hydrophobic effect—a clear consequence of their aqueous environment. Water contributes to the mechanism responsible for membrane/membrane interaction and contributes to the assisted passage of ions and other molecules across biomembranes through special membrane-embedded proteins. Since natural biomembranes represent complicated assemblies of molecules, their study is extremely involved. To simplify the task, the properties of biomembranes are often probed using model membranes containing one type of phospholipid molecule or a simple mixture of lipid molecules.

Different experimental techniques are used to study properties of model membranes and their hydration water. The structural properties of membranes and the positions of lipid fragments and hydration water can be measured with the help of X-ray and neutron scattering techniques.[1,2] Neutron scattering has also proved to be very useful in the study of the interaction between biomembranes and their hydration water.[3] NMR spectroscopy emerged as one of the most important tools used for the study of a large variety of issues related to changes in the structural and dynamical properties of membranes due to membrane hydration. Examples of issues probed by NMR include headgroup conformational changes as a function of the water hydration level,[4] permeation of water across the membrane,[5] and dynamical properties such as water residence times.[6] Infrared spectroscopy[7] can provide information on the hydrogen bonding between water and biomolecules, and fluorescence spectroscopy can probe the dynamics of water molecules in the hydration shell.[8] To study interactions between membranes and how properties of water in the interbilayer spaces influence these interactions, osmotic stress[9] and humidity-controlled osmotic stress techniques are used.[10] The thermodynamics of hydration are studied using new calorimetric methods that allow for separate determination of the energetic and entropic contributions to the dehydration process.[11] A more detailed overview of these techniques is provided in a recent excellent review on the water/phospholipid model membrane interactions written by Milhaud.[12]

In addition to the above-mentioned experimental techniques, computer simulation techniques that employ molecular dynamics and/or Monte Carlo methods are also applied toward the study of structural and dynamical properties of model membranes and their hydration water.[13−23] The first full molecular detail simulation done on a system consisting of a bilayer containing a mixture of ternary alcohol with fatty acid and its solvating water was performed by Egberts and Berendsen in 1988.[24] Full molecular detailed simulations of phospholipid bilayers solvated in water were performed in the early nineties (see ref 13 for a detailed review of this earlier work). At the present time, there exists a vast amount of literature that deals with computer simulation studies of biomembranes, and it is probably not even possible to summarize all the work described in this literature in one review. Therefore, we will limit our discussion to the subject of computer simulation studies of the aqueous-solution/model-biomembrane interface since this aspect of the recent

* To whom correspondence should be addressed. E-mail: maxb@unc.edu. Telephone: 919-962-1218. Fax: 919-962-2388.
† Current location: The Scripps Research Institute.
‡ Current location: The Illinois Institute of Technology.

10.1021/cr0403638 CCC: $59.00
Published on Web 02/09/2006

Max L. Berkowitz was born in Chernovtsy, Ukraina (former Soviet Union), in 1950. He obtained his M.Sc. in Physics from Novosibirsk State University, Russia, in 1972 and his Ph.D. in Physical Chemistry from Weitzman Institute of Science, Israel, in 1979. He was a postdoctoral fellow at Purdue University with Professor Steve Adelman developing a description of chemical processes using the generalized Langevin equation. In 1980–1983 he was a Visiting Assistant Professor at the University of Houston working in the group of Professor J. A. McCammon. During this period he learned molecular dynamics methodology and studied the properties of aqueous solutions. In 1983 he joined the Department of Chemistry at the University of North Carolina at Chapel Hill, where he continued his studies of aqueous solutions in bulk, in clusters, and next to surfaces. His research centers on understanding of properties of biomembranes using computational methodologies such as molecular dynamics.

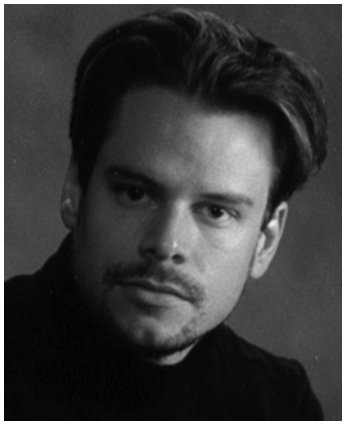

David Bostick was born in Bloomington, Indiana, in 1975 and was raised in Raleigh, North Carolina. He obtained his B.Sc. in Physics with emphases in Mathematics and Chemistry from The Appalachian State University in 1998. He then moved on to obtain his Ph.D. in Physics with an emphasis in Biochemistry and Biophysics at The University of North Carolina at Chapel Hill. There, his work focused on understanding biological membrane structure and assembly and ion channels in aqueous solutions by utilizing computational methods. David's research interests range from biomembranes, ion channels, and ionic solvation to structural proteomics and methodological developments in computational approaches to understanding complex molecular and biological systems. Currently, David is a National Science Foundation Postdoctoral Fellow in Biological Informatics, performing his research at The Scripps Research Institute in La Jolla, California.

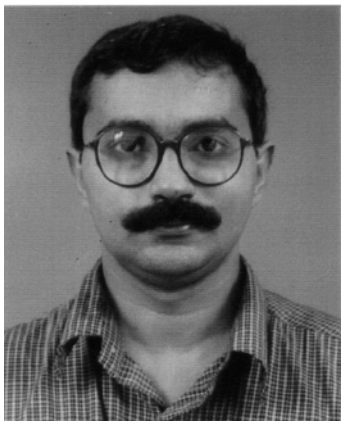

Sagar Pandit was born in Ravalgaon, India, in 1968 and was raised in Mumbai (Bombay), India. He obtained a B.Sc. in Physics with emphases in Mathematics and Chemistry from Parle College, Bombay University (India), in 1989. He then moved on to obtain his M.Sc. and Ph.D. in Mathematical Physics at The University of Pune in Pune, India. In Pune, his research was on the theory of dynamical systems. Later, during postdoctoral work at the University of North Carolina at Chapel Hill and Illinois Institute of Technology in Chicago, his focus shifted to understanding biological membrane structure and assembly in aqueous solutions and structural properties of heterogeneous membrane systems by utilizing computational methods. Sagar's research interests are in biomembranes, mathematical modeling of complex biological and social systems, dynamical systems, and computational approaches toward addressing problems in these fields. Currently, Sagar is at Purdue University as a research associate.

work was described very briefly in the Milhaud's review. In this respect one can consider our review as complementary to the review by Milhaud.

2. Hydration Force

The structure of water next to the biomembrane surface and its role in the interaction between biomembranes were actually among the first issues investigated in the initial simulations performed on model biomembranes in the early nineties.[25−29] Experimental studies that used osmotic stress techniques demonstrated that the force of interaction acting between model membrane surfaces containing molecules such as dipalmitoylphosphatidylcholine (DPPC) is repulsive and that the decay of this force has an exponential character[9]

$$P = P_0 \exp(-x/\lambda) \quad (1)$$

with the decay exponent λ having a value in the range 0.1−0.3 nm. The fact that the value of λ is close to the size of a water molecule, naturally, triggered the idea that interbilayer water is responsible for this force, and therefore, it was called the "hydration force". Accordingly, it was assumed that the origin of the force was due to the removal of structured water between lipid bilayers, which requires work to be done and therefore results in an increase of free energy as the distance between bilayers decreases.

At the same time, another explanation for the origin of the hydration force was proposed: the force is due to steric interactions between the headgroups of lipid molecules that protrude from the surfaces.[30] A series of theoretical papers investigated the nature of the hydration force, providing arguments in favor of one or the other point of view.[30−41]

McIntosh and Simon performed a series of experiments using substitutions in the structure of lipid molecules to study the nature of the hydration force acting between bilayers.[42] The results of their experiments demonstrated that the hydration force has three regimes. The first regime is at large distances, where the force depends on the phase of the lipid bilayer and is mostly due to interactions between undulating membrane surfaces. In the second regime, when the distance between membrane surfaces is in the region 0.4−0.8 nm, the force is independent of the lipid phase, and therefore, according to McIntosh and Simon, the force is indeed due to the presence of water molecules. In this regime there are

roughly two to three layers of water that separate membrane surfaces. Finally, in the third regime, when the distance between bilayers is below 0.4 nm, steric interactions between headgroups play the dominant role. These observations indicated that the part of the hydration force due to water is short ranged and that the effect of the surface on the structure of water propagates only one to two layers away from the surface. Indeed, later simulations of Essmann et al.[43] were in agreement with the conclusions of McIntosh and Simon.

3. Structural and Dynamical Properties of Hydration Water

3.1. NMR Experiment and Simulations

How many water molecules belong to the hydration shell of lipids? Heavy water NMR together with molecular dynamics simulation techniques can help answer this question. In NMR experiments one measures quadrupolar splittings that are proportional to water orientational order parameters. In their turn, the orientational order parameters tell us the average orientation of the angle *b* between the OH vector of the water molecule and the interface normal. Specifically, the quadrupolar splitting is proportional to the second orientational order parameter *S* given by the following expression:

$$S = \left\langle \frac{1}{2}(3\cos^2\beta - 1) \right\rangle \quad (2)$$

Comparison between the properly averaged and weighted values of *S* measured by NMR experiment and the values of *S* obtained from simulations can produce a large amount of insightful information about interfacial water. Such a comparison was performed recently by Aman et al.[44] They concluded that there are ~17 water molecules that are perturbed by the DPPC headgroup. They also observed that the order parameter distribution within the bilayer/water interface reveals two types of interfacial water molecules: those with positive order parameter that tend to have their dipoles flat in the membrane plane, and those with negative order parameter that orient their dipoles along the bilayer normal. From the molecular dynamics simulations Aman et al. also obtained information on the dynamical properties of hydration water. They found that the water reorientation correlation function has a part that shows a fast initial decay when the water molecules stay localized and a part that slowly decays. The slowly decaying part is due to the motion of water molecules along the interface. Although the simulation of Aman et al. was one of the longest and largest simulations of its time, still it was limited in its time and length domains (100 ns, 4−5 nm size). Therefore, it was not able to describe correctly large-scale motions and explain the character of slow modes of motion observed in NMR experiments.

3.2. Classification of Interfacial Hydration Water

In the simulations of Aman et al., water molecules in the bilayer hydration region were classified according to the sign of their orientational order parameter. Jedlovszky and Mezei also used the orientational ordering of water molecules at the water/bilayer interface as a criterion for their classification.[45] Usually, a density profile is used to classify waters, although in the case of a rough surface the task is not as simple as in the case of water next to a smooth surface.

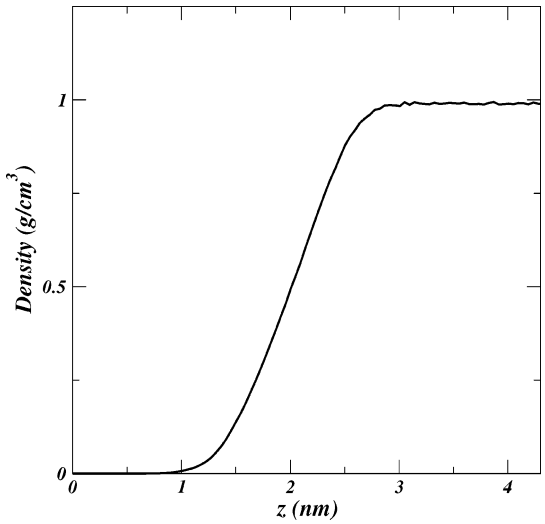

Figure 1. Local density of water as a function of the distance from the DPPC bilayer center. The *z*-axis is taken along the bilayer normal.

If one calculates the density profile of a liquid next to a smooth or slightly corrugated surface, one observes an oscillatory profile of this density. The free energy as a function of distance to the surface and, therefore, the force of interactions between relatively smooth surfaces immersed in a liquid will also have an oscillatory profile and, therefore, will reflect the packing structure of the liquid against the surface walls. This can be seen, for example, from the results of a surface force apparatus experiment, which measures the interactions between mica surfaces immersed in the nonpolar liquid octamethylcyclotetrasiloxane, a liquid consisting of nonpolar spherical molecules.[46]

The observed smooth nonoscillatory behavior of the hydration force acting between biomembrane surfaces is a reflection of a "wash-out" of such an oscillatory structure due to a broad interface between water and the biomembrane surface. The broad character of the interface can be seen from Figure 1, where water density as a function of the distance from the middle of the bilayer is depicted. Figure 1 shows that water density smoothly increases from zero to the bulk density value over a range of ~2 nm. Although water density displays a smooth profile when plotted as a function of the distance from the bilayer center, there is still structure in the water. This "structural obfuscation" of water has been observed at water/oil interfaces and has been resolved by proximal density distribution functions.[47] The structure of water can also be recovered when the local water density is plotted as a function of the distance to the bilayer surface. To find the distances between water molecules and the rough bilayer surface, we need to use some form of a geometric construction that will describe the surface. While a solution of this task is elementary for a smooth surface, it is somewhat involved in the case of a rough lipid membrane surface. One of the possible ways to achieve this task was proposed by Pandit et al.[48] According to Pandit et al., the rugged membrane surface can be treated approximately as an assembly of "patches". To quantify the distance between a water molecule and this approximated surface, the quantity *d* (distance from the surface) was obtained using the following procedure:

1. Since the system geometry is planar, the coordinates of the chosen atoms of the lipid molecules were projected

Table 1. Properties of Classified Water in Regions near the DPPC Membrane Surface[a]

	I	II	III, IV	V
ρ_{av} (g/cm^3)	0.169	1.031	0.982	0.985
N_w (no. of waters/lipid)	6.6	6.0	13.0	25.7

[a] The average density of water and number of water molecules per lipid in each region near the membrane surface as classified in Figure 2.

onto the plane with $z = 0$ that goes through the center of the bilayer.

2. A Voronoi tessellation of the $z = 0$ plane with the projected coordinates of the chosen lipid atoms at the centers of the polygons was performed.

3. The coordinates of the water molecules onto the $z = 0$ plane were also projected.

4. A water molecule is associated with a Voronoi simplex if the projected coordinates of the water oxygen fall in the interior of that simplex.

5. The simplexes are then lifted to the z coordinates of their corresponding lipid atoms. The distance from the surface of the bilayer, d, is defined as the distance between the z coordinate of the water oxygen and the z coordinate of the corresponding lifted Voronoi simplex.

In the initial work of Pandit et al., phosphorus atoms of the lipid molecules were chosen as centers of Voronoi polygons. This produced a rather "crude" description of the membrane surface. Nonetheless, based on local density alone, Pandit et al. obtained a classification of water near the membrane surface similar to that determined using water orientation by Aman et al. Using their classification method, Pandit et al. predicted that 19.5 waters per lipid were perturbed, which is similar to Aman's ~17 waters per lipid. A more refined description of the membrane surface can be achieved when the coordinates of both phosphorus and nitrogen atoms of lipid headgroups are projected onto the $z = 0$ plane. With this more refined classification it was determined that approximately 25 water molecules per lipid were perturbed (see Table 1), in accordance with the number received from calorimetric measurements.[49]

After the more detailed "patched" surface is constructed and the distances d for the water molecules from this surface are calculated, one can obtain the number density of water as a function of the distance from the "patched" plane. In this case, it is expected that the water density plot will display an oscillatory character that will reflect the hidden packing arrangement of water against the surface of the lipid membrane. Such oscillations indeed appear on a plot of the water density as shown in Figure 2. The oscillations make it possible to separate hydration water into different layers. These are layers corresponding to water inside the membrane, water in the primary hydration shell, water in the secondary hydration shell, and finally bulk water. In addition to the water density, the lipid density is also displayed in Figure 2. On the basis of these two density plots, water molecules in the simulation box are assigned to different regions that depend on the distance of water oxygen to the membrane surface.

The membrane surface can be placed at the position where the density of lipids reaches zero, while $d = 0.0$ nm represents the position of the surface formed by the phosphorus and nitrogen atoms of the DPPC molecules. The classification of water molecules now can be done in the following way: all the water molecules with the d coordinate

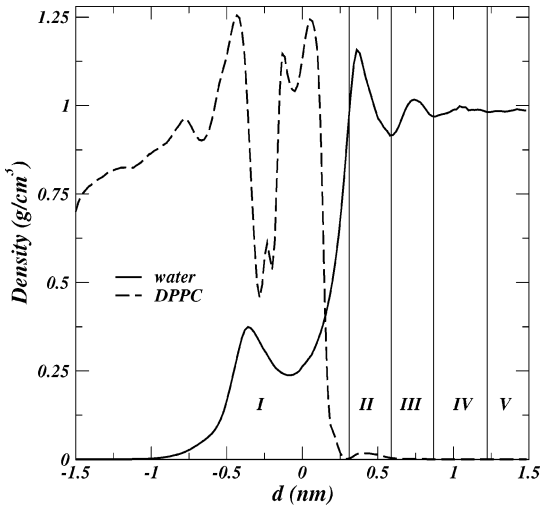

Figure 2. Density of water and lipid with respect to the rugged molecular surface defined by the phosphorus and nitrogen atoms of the DPPC bilayer lipid headgroups. The plot reveals the locations of buried water (region I) near backbone and carbonyl groups, a first external shell (region II) near the phosphocholine group, secondary shells (regions III−IV), and bulk water (region V).

less than $d = 0.31$ nm (where the density of the DPPC bilayer goes to zero) belong to region I. These are the water molecules that penetrate the membrane. All simulations dealing with the membrane/water interface show a substantial penetration of water molecules into the headgroup region up to the ester groups. The borders between other regions are determined by the minima in the water density plot. Those water molecules that have their distances between the values $d = 0.31$ nm and $d = 0.59$ nm belong to the primary hydration level of the membrane (region II). Note that region II is roughly the size of a single water molecule. There are two other regions that show oscillations in water density (these regions correspond to secondary hydration water). They are denoted as regions III (0.59 nm $< d <$ 0.87 nm) and IV (0.87 nm $< d <$ 1.22 nm). Finally, the remaining water displays bulklike properties. The density of water and number of water molecules per lipid in the corresponding regions is shown in Table 1. As we can see from this table, there is a slight increase of the water density (~3%) in the primary hydration region. This increase in density next to bilayers was also inferred from experiments.[50] The increase in water density can be explained as due to a simple packing arrangement, just as in the case of water next to a plane wall.

The methodology we outlined here of classifying water near the surface gives us a way to understand and quantify what is already known experimentally. For example, experimental work has been able to determine that water penetrates deeply into the surface at the bilayer/aqueous solution interface.[51,52] Via simulation combined with methodologies such as this, the extent to which the water penetrates, and where it is located, can be described.

3.3. Hydrogen Bonding of Interfacial Hydration Water

The change in density of water described above has consequences on the water hydrogen bonding structure and on the dynamics of water molecules in the primary hydration shell. Molecular dynamics simulations that studied the hydrogen bonding structure of water next to the DMPC lipid bilayer surface were initially performed by Pasenkiewitz-

Gierula et al.[53,54] Since these initial simulations were of limited statistics, Lopez et al. reexamined water at the DMPC bilayer surface, also using molecular dynamics simulation techniques.[55] Lopez et al. found that ester oxygen atoms have a smaller probability to form a hydrogen bond than carbonyl oxygen atoms. They also observed that the oxygens of the phosphate group are strongly engaged in hydrogen bonding due to their extensive contacts with water. While the highest probability (74%) for the formation of one hydrogen bond was observed for double bonded oxygens connected to phosphorus atoms, the singly bonded oxygens connected to phosphorus had a smaller probability to be engaged in one hydrogen bond (18% and 27%). Since water penetrates up to the carbonyl groups, the oxygens of these groups also participate in hydrogen bonded interactions with water. The carbonyl oxygen atoms in the tails had a 43% chance to be engaged in one hydrogen bond, while the ester oxygens in the tails had a very small chance (7% and 2%) to participate in one hydrogen bond with water.

Radial distribution functions (rdf's) were calculated for water oxygens around different reference atoms of lipids to show the details of the water structure. These rdf's were augmented by the three-dimensional distribution functions (3ddf's) of water around these reference atoms. The rdf and 3ddf for water/nitrogen pairs showed that water surrounds the choline group in two well defined solvation shells. The water/phosphorus rdf and 3ddf demonstrate that the phosphate group is primarily solvated by water molecules in contact with singly bonded oxygens.

Water molecules that serve as bridges between water molecules solvating the singly bonded oxygens were also observed. Lopez et al. found that most lipid molecules will utilize hydrogen bonding bridges. The presence of such bridges contributes to structural properties of the water/membrane interface. In general, they concluded that the combination of hydrogen bonding, hydrogen bonded bridges, and charge-pair interactions form a network at the interface that determines the stability, structure, and dynamics of this interface. Note that although qualitative conclusions on the hydrogen bonding pattern are not very sensitive to the exact definition of the hydrogen bonding event, quantitative results are sensitive to such definitions. In the work of Lopez et al. the following definition for the hydrogen bonding was adopted: a hydrogen bond between any two oxygens was said to exist when the oxygen−oxygen distance is less than 0.325 nm and the angle between the O−O vector and the O−H bond is less than 35°.

To study the hydrogen bond dynamics, Lopez et al. calculated the time dependent correlation function,

$$c(t) = \frac{\langle \chi(0)\chi(t)\rangle}{\langle \chi^2(0)\rangle} \tag{3}$$

where $\chi(t)$ is the progress variable, which (for a given time, t) is equal to 1 if a water oxygen and a lipid oxygen are hydrogen bonded and is equal to 0 otherwise. The correlation function, $c(t)$, gives the probability that the hydrogen bond formed at $t = 0$ is still intact at time t. Lopez et al. observed that hydrogen bonds between water and double bonded lipid oxygens are longer lived than those between water and single bonded lipid oxygens and that hydrogen bonds between waters and the tail lipid oxygens are longer lived than those to headgroup oxygens.

Lopez et al. found that the kinetics of hydrogen bonding in water at the lipid surface was qualitatively very similar to the kinetics observed by Luzar and Chandler,[56,57] who used eq 3 to study the kinetics of hydrogen bonding in bulk water. Lopez et al. also studied the translational diffusion of water next to the lipid molecules and observed that it slowed. For example, the value of the diffusion coefficient for water molecules associated with the headgroup oxygens was calculated to be $\sim 2.0 \times 10^{-7}$ cm^2/s, while in the bulk it was roughly 2 orders of magnitude faster ($\sim 4 \times 10^{-5}$ cm^2/s).

4. The Dipole Potential

4.1. Experimental Measurements

Biological membranes are not just simple barriers that separate cells from the surrounding media. They also regulate many functions of the cells, including the exchange of matter and information between cells and their environment. For example, transport of the ions into and out of the cell is made possible by the existence of proteins embedded into the lipid bilayer. In many cases the transmembrane electrical potential $\Delta\Psi$ regulates the function of such proteins.

The electric potential Ψ at any point is determined by the distribution of ions in the bathing electrolyte solution, the distribution of charges on the lipid headgroups if and when the lipids are charged, and, finally, the distribution of dipoles at the membrane/water interface. While charges produce the surface potential Ψ_s, dipoles are responsible for the dipole potential Ψ_d. The value of Ψ_d cannot be measured directly, and therefore, it has to be inferred from indirect experimental methods. For saturated phospholipid membranes, this value is in the range 220−280 mV and it is positive in the interior of the membrane.[58] Although this change in the potential may not seem to be very large, it occurs over a distance of 1 nm and therefore produces a very strong electric field at the interface—a field in the range of $2-3 \times 10^8$ V/m. A field of this value will play an important role in determining processes that involve motion of charged species at the water/membrane interface.

The role and the importance of Ψ_d were discovered in 1969 when it was observed that certain hydrophobic ions could diffuse directly across the bilayer.[59] It was also observed that the specific conductance of anions is very different compared to that of cations. Consider, for example, tetraphenylborate (TPB^-) and tetraphenylarsonium (TPA^+) ions that differ in their charge but otherwise are similar in size and chemical structure. From the measured ratio of their specific conductances it is possible to infer the value of the dipole potential through the following expression:

$$\Psi_d = \frac{RT}{2F} \ln \frac{g_{TPB}}{g_{TPA}} \tag{4}$$

where R is the gas constant and F is the Faraday number. To arrive at eq 4, a number of assumptions must be made.[60] Therefore, the measured value of the dipole potential is strongly dependent on the validity of such assumptions. One of the key assumptions made in deriving eq 4 is the assumption that the nonelectrostatic free energy change in moving the ion across the interface is the same for the cation and anion. A small difference in the free energies such as 20 kJ/mol will change the dipole potential by a value of 104 mV. Spectroscopic methods also exist for the detection of the dipole potential.[61]

While the measurement of dipole potential for a bilayer is done using an indirect method, it is possible to use a more

direct electrochemical method to measure the potential difference across a monolayer.[62] If one assumes that a monolayer represents half of a bilayer, the measured potential represents a good estimate of the potential in the bilayer. Nevertheless, the comparison between monolayer and bilayer is not that simple. Both bilayer and monolayer should be in corresponding states.[63] Moreover, the measurements performed on monolayers are not completely direct either, since the potential in this case is measured relative to a reference state, such as a clean water/air interface. In general, one finds a discrepancy of ~100 mV in the value of dipole potentials measured from corresponding experiments performed on monolayers and bilayers.

There must be a connection between Ψ_d and the hydration force, since both of them originate from the reorientation of water at the interface. It was proposed that phospholipid headgroups create a hydration potential Ψ_h, which is proportional to the value of the hydration force. Later it was assumed that Ψ_h can be identified with the dipole potential Ψ_d, thus directly coupling the hydration force and the dipole potential.[64] Unfortunately, a number of unresolved theoretical and experimental issues still prevent us from the quantitative understanding of this connection. For a more detailed description of the dipole potential measurements, issues associated with these measurements, and their connection to the hydration force, the reader is referred to the review by Brockman.[63]

4.2. Measurements Obtained from Simulations

Computer simulations present one of the nicest tools to study the dipole potential. If the simulation is performed on a system containing an uncharged lipid bilayer and water, it is the dipole potential that is responsible for the difference in the potential between the middle of the bilayer and the middle of the bathing slab of water. Since the system has planar symmetry, the dipole potential can be obtained from double integration of the Poisson equation and, therefore, is given by the following expression:

$$\Psi(z) - \Psi(0) = -\frac{1}{\epsilon_0}\int_0^z dz' \int_0^{z'} dz'' \, \rho(z'') \qquad (5)$$

where $\Psi(z)$ is the dipole potential at point z, $\Psi(0)$ is the dipole potential in the middle of the bilayer, and $\rho(z)$ is the excess charge density at point z. Simulations performed on different phospholipid bilayers in different groups using different force fields show qualitative agreement with experiment (the potential is positive in the middle of the bilayer), although quantitative agreement is not always achieved. For example, in simulations performed on DPPC bilayers, the dipole potential has a value of ~600 mV,[65] which is larger than the value of the dipole potential inferred from experiment. This discrepancy between the calculated and measured values of the dipole potential was also observed in other simulations.[14,66−68] It was even suggested by Berger et al.[69] that calculations of the value of the dipole potential can be used to calibrate the values of headgroup charges used in the simulations.

4.3. Where Does the Dipole Potential Come From?

The nice feature of the simulations is that one can find out the contributions of different groups or molecules to the total value of the dipole potential. All simulations show that the sign of the dipole potential is determined by overcompensation of water molecules over the dipoles of the lipid headgroups. Figure 3 shows a simulation-derived plot of the dipole potential as a function of the distance from the bilayer center and separate contributions to this potential from lipid and water molecules. The overcompensation effect can be clearly seen from this figure. The potential due to lipids has a different sign than the potential due to water molecules, and the water potential has a higher value. One can also determine which specific moieties of the lipid headgroups and which specific regions of hydration water contribute most to the value of the dipole potential. According to Pandit et al.,[48] these are the phosphate group and its hydration water. This agrees with the conclusion reached in the experimental study by Gawrish et al. that the first layer of water molecules at the lipid/water interface makes the major contribution to the dipole potential.[70]

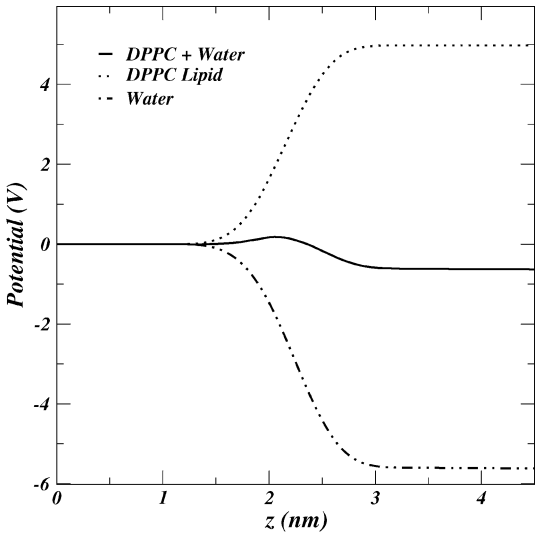

Figure 3. Electrostatic potential due to various components of the membrane as a function of the distance from the center of the DPPC bilayer. The *z*-axis is taken along the bilayer normal.

The sign of the total dipole potential, which is determined by the balance between the contributions from the phospholipids and water, depends on the amount of hydration water. Mashl et al.[71] simulated an uncharged zwitterionic phospholipid bilayer containing dioleoylphosphatidylcholine (DOPC) molecules at different levels of hydration. They showed that the sign of the dipole potential changes with the amount of hydration water present in the system. A small amount of hydration water undercompensated the dipole contribution from lipid headgroups.

5. Ionic Aqueous Solutions at Membrane Surfaces

Since biological membranes are charged entities, aqueous solutions next to these membranes contain ionic species: counterions and electrolytes. The interactions between membranes or between membranes and peptides strongly depend on the electrostatic properties of the system,[72−75] and these, obviously, depend on the presence of ions and their specificity. The specific effect of ions on the properties of biomolecules was first discovered in the study of the propensity of ions to salt-out proteins from aqueous solution. The action of ions can be arranged in a series, which is today known as the Hofmeister series.[76] Although it is understood

that the Hofmeister series plays an important role in colloidal science and biology, the nature of this series is still not completely understood.[77−82]

Two competing hypotheses exist that attempt to explain the effect. The first hypothesis presumes that the series is due to the specific ionic ability to break or make a hydrogen bonding network in water (chaotropic vs kosmotropic behavior).[77,79] The second hypothesis assumes that the dispersion interaction between the ion and the surface plays the major role and determines the behavior predicted by the series.[80] Whatever the reason for the Hofmeister effect, it is clear that the distribution of ions in the solution, the interaction of ions with water and solutes, and the ion/ion interactions are the factors that contribute to the specificity of the effect.

5.1. Simple Electrostatic Model Employing a Continuum Solvent Description

The electrostatic properties of ionic aqueous solutions next to surfaces can be studied using different levels of models. The simplest model considers the electrolyte solution as a dielectric continuum described by the dielectric constant ϵ with point ions embedded in the continuum. The surface is represented by a smooth charged wall with a homogeneous charge density, σ. Usually this model is described in terms of the Poisson−Boltzmann (PB) approximation. Recent work of Netz and collaborators provided a more complete picture of the electrostatics in our simple model.[83−85] The treatment is quite involved, but the main ideas can be discussed using scaling arguments. First, consider a Hamiltonian of the problem written in units of kT It has the form

$$\mathcal{H}kT = \sum_{j=1}^{N-1}\sum_{k=j+1}^{N}\frac{q^2 l}{r_{ij}} + 2\pi q l \sigma \sum_{j}^{N} z_j \qquad (6)$$

where $l = e^2/4\pi\epsilon_0\epsilon kT$ is the Bjerrum length, which is ∼0.7 nm in water at 300 K.

Now introduce another length scale μ,

$$\mu = \frac{1}{2\pi q l \sigma} \qquad (7)$$

which is called the Gouy−Chapman length. If we measure all the distances in terms of the Gouy−Chapman length, the Hamiltonian in new scaled coordinates will be

$$\mathcal{H}kT = \sum_{j=1}^{N-1}\sum_{k=j+1}^{N}\frac{\Gamma}{\tilde{r}_{ij}} + \sum_{j}^{N}\tilde{z}_j \qquad (8)$$

where $\tilde{z} = z/\mu$ and $\tilde{r}_{ij} = r_{ij}/\mu$ are the scaled distances. The scaled Hamiltonian depends on a single parameter Γ

$$\Gamma = 2\pi q^3 l^2 \sigma = q^2 l/\mu \qquad (9)$$

called the coupling parameter. Note that the coupling parameter is small when the surface charge density is small and when the ions are monovalent. It can be shown that for any Γ the typical distance of an ion from the wall is $\sim\mu$, and this distance is ∼1 in reduced units.

Finally let us introduce one more distance, a, which is the average lateral distance between ions. This distance satisfies the relationship

$$\pi a^2 = q/\sigma \qquad (10)$$

In reduced units we get for $\tilde{a}$

$$\tilde{a} = a/\mu = \sqrt{2\Gamma} \qquad (11)$$

When the coupling parameter $\Gamma > 1$, the lateral separation between ions is larger than the separation between the ion and the wall, and therefore, the ionic layer is essentially flat and two-dimensional. When $\Gamma < 1$, the lateral separation between ions is smaller than the average ion−wall distance and the ionic layer is three-dimensional.

Netz and collaborators showed that when Γ is small (in the so-called weak-coupling limit) the mean-field or Poisson−Boltzmann theory is valid, since in this case every ion interacts with a diffuse cloud of other ions. Contrariwise, in a strong-coupling limit, when Γ is large, every ion is moving independently along the vertical direction and does not interact with the mean field from other ions. In this case, the Poisson−Boltzmann theory is not applicable. The exact criteria for the validity of the weak-coupling and the strong-coupling limits are given in the work of Netz.[83]

A simple model of two interacting homogeneously charged surfaces imbedded in the dielectric continuum containing counterions can be used to understand the electrostatic interaction between charged macromolecules such as DNA or the interaction between charged membranes. Consider, for example, the interaction between bilayers containing charged dioleoylphosphatidylcholine (DOPS) lipid molecules with Na^+ counterions immersed in water. This system was recently studied by Petrache et al.[86] If we approximate the bilayers as charged plates with an area per unit charge of ∼0.7 nm^2, we get that $\mu = 0.16$ nm and $\Gamma = 4.4$. Can one use the PB theory in this case? According to the detailed arguments given by Netz,[83] the PB approximation is valid when the reduced distance between the plates is large ($\tilde{d} > 1$) and the criterion

$$\Gamma < \tilde{d}/\ln(\tilde{d}) \qquad (12)$$

is satisfied. Using our parameters, the criterion (eq 12) is satisfied for distances between plates that are larger than 1.6 nm, and therefore, the use of the PB equation is justified for these distances. Indeed the data on the interaction between DOPS membranes were successfully explained by the application of the PB theory when the distances between membranes were in the range 2.0−10.0 nm.[86]

Now consider another case where two charged macromolecules or two charged membrane surfaces are separated by a distance d, and the counterions are divalent Ca^{2+} ions. Assuming that the surface charge density is the same as that in the DOPS case, we obtain the values $\mu = 0.08$ nm and $\Gamma = 35.2$. Therefore, the criterion in eq 12 is not satisfied for distances in the above-mentioned range of 2.0−10.0 nm. As a matter of fact, it is possible to show that SC theory can be applied in this situation at distances $d < 1.16$ nm, but at these distances the detailed molecular character of membranes and aqueous solution starts playing an important role.

In some cases, PB theory predicts not only a quantitatively incorrect result but also a qualitatively wrong one. For the interaction between two charged surfaces, PB theory always predicts a repulsive interaction between surfaces. As the detailed analysis shows,[83] the SC limit will predict an attraction caused by the presence of counterions when the

distance between surfaces is smaller than the average lateral distance between ions.

5.2. Simulations with Explicitly Treated Water

Both SC and PB theories describe water as a dielectric continuum, and this may be inappropriate if a quantitative description of a problem is required, especially when the distance between two interacting surfaces of biomolecules is only a few times the diameter of the water molecule. The difference in electrostatics when water is considered as a continuum and when it is described explicitly can be seen from the results of simulations performed by Pandit and Berkowitz[87] and also by Lin et al.[88] Pandit and Berkowitz simulated a system containing water and Na^+ ions embedded between bilayers of dipalmitoylphosphatidylserine (DPPS) lipid.[87] A continuum model, in both SC and PB limits, predicts that the electrostatic potential is negative at the interface and decays to zero toward the bulk aqueous phase. As one can see from Figure 4, the simulation showed that the electrostatic potential was positive at the bilayer/water interface and decayed to zero in the bulk aqueous phase. It also showed that a very large proportion of Na^+ ions were "adsorbed" to the bilayer. The ions were situated in close proximity to serine groups, thus compensating their charge. Since the remaining part of the DPPS molecule is very similar to the dipalmitoylphosphatidylethanolamine (DPPE) molecule, some of the properties of the DPPS bilayer in the presence of the Na^+ counterions are similar to the properties of DPPE bilayers.

As we already mentioned, water next to a neutral zwitterionic bilayer such as DPPC or DPPE overcompensates the field due to the dipoles in the bilayer. The resulting total potential produced is positive when moving from the water phase to the bilayer phase. Lin et al. observed in their simulations on hydrated zwitterionic palmitoyloleoylphosphatidylcholine (POPC) bilayers that the membrane dipole potentials strongly depended on the way water was treated: explicitly or implicitly. They observed that calculated dipole potentials converged when four or more hydration layers containing explicitly described water were included in the calculation.

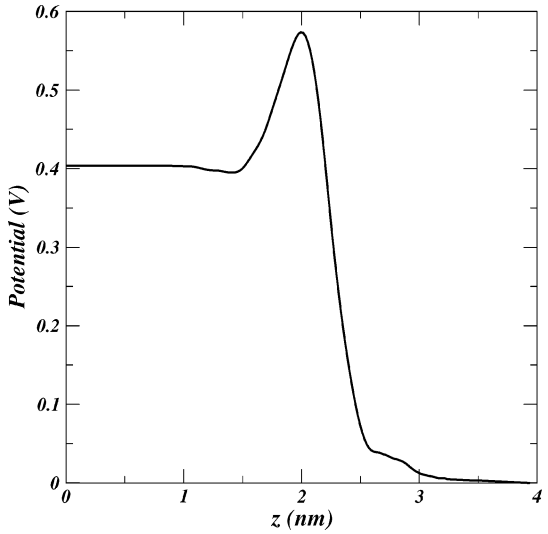

Figure 4. Electrostatic potential from the simulation of a hydrated DPPS membrane with Na^+ counterions. The potential is seen to be positive in the interfacial region, 1.8−2.5 nm from the center of the bilayer.

5.3. Experimental Studies of Ion Binding to Membrane Surfaces

Since ions modulate the interactions between biomembranes and other biomolecules, their location at the interface between biomembranes and aqueous solution is an important issue that has attracted close attention. As a result, a number of experimental studies were performed to investigate this issue. Thus, adsorption of monovalent cations to membranes containing negative phospholipids was studied by McLaughlin and collaborators.[89] They measured electrophoretic mobilities of multilammelar phosphatidylserine vesicles in solutions containing monovalent cations such as lithium, sodium, ammonium, potassium, rubidium, cesium, tetraethylammonim, and tetramethylammonium chloride. The electrophoretic mobility change was also studied in order to understand the effect of phase transitions on the binding of anions to dimyristoylphosphatidylcholine (DMPC) liposomes.[90] Deuterium and phosphorus-31 NMR were used to study binding of anions to neutral and positively charged lipid membranes[91] and interactions of metal ions with phosphatidylcholine bilayers.[92] A fluorescent ratio method using dyes was applied to study the influence of ions on the properties of dipole potentials.[60] More recently, infrared spectroscopic methods were used to study the effect of metal cations on the hydration of zwitterionic membranes such as POPC.[93]

All experimental evidence points to an existence of specific interactions between ions and membrane surfaces. The detailed description of these interactions is hard to obtain from most of the experiments; therefore, simulations should be able to help in understanding the specificity of the ionic binding and its possible connection to the Hofmeister series.[60,80] Recently, a number of simulations appeared, where charged or neutral bilayers were immersed in the aqueous solutions containing salts and/or counterions.

5.4. Specific Interactions of Ions with Charged Membranes

As we already mentioned, Pandit and Berkowitz simulated bilayers of DPPS separated by water containing Na^+ counterions.[87] Mukhopadhyay et al.[94] performed two simulations with palmitoyloleoylphosphatidylserine (POPS) bilayers: one was in the presence of Na^+ counterions only, and the other contained Na^+ counterions and NaCl salt. These simulations were done using a constant pressure ensemble, and therefore, the area per headgroup was allowed to fluctuate. Unexpectedly, the average area per headgroup from the simulations performed on POPS systems by Mukhopadhyay et al. came out to be nearly the same as the area per headgroup from the simulation performed on the DPPS system by Pandit and Berkowitz. POPS is an unsaturated lipid, and therefore, it is expected that its area per headgroup will be larger than the area per headgroup in a bilayer containing saturated lipids. Although the simulations of the POPS systems were performed at 300 K, while the simulation on DPPS was performed at 350 K, the transition temperature for DPPS is 327 K, while it is 287 K for POPS, and therefore, the temperature difference in the simulations should not play an important role. There also was a difference in the length of the molecular dynamics runs. While Pandit and Berkowitz performed their analysis using data from a 4 ns run after a few nanoseconds of equilibration time, the analysis in the work of Mukhopadhyay et al. was done for 25 ns after a

15 ns equilibration time, which was required to reach a stable area value. Pandit and Berkowitz observed that Na^+ ions were located next to carboxylate groups, while Mukhopadhyay et al. observed that Na^+ ions moved more toward the membrane interior and were situated next to ester carbonyl oxygens. The coordination of Na^+ ions with headgroup oxygens was accompanied by a simultaneous loss of water in the ions' coordination shells. Mukhopadhyay et al. observed that addition of NaCl salt increased the number of Na^+ ions that penetrated deeper into the membrane. The ionic density plots from the simulations of Mukhopadhyay et al. indicated that Cl^- ions did not substantially penetrate into the membrane.

5.5. Specific Interactions of Ions with Zwitterionic Membranes

Systems containing neutral bilayers in the presence of monovalent salts were also simulated recently. Pandit et al.[95] studied a system containing a DPPC bilayer and an aqueous solution of NaCl and compared the results of this simulation with the result of a simulation on pure DPPC. The arrangement of lipids and electrolyte in this simulation is shown in Figure 5. The lengths of the simulated runs that were analyzed in this work were 5 ns each. The results showed that addition of salt to a DPPC bilayer slightly decreased the area per headgroup. Pandit et al. observed that many Na^+ ions were tightly bound to the lipids, creating ion lipid complexes containing on average two lipids per ion. The complexes were coordinated through phosphate and carbonyl portions of the lipid headgroups. Somewhat unexpectedly, Cl^- ions were only very slightly bound to lipids and the separation between the peaks in the distributions of the ions was quite wide, having a value of ~1.2 nm.

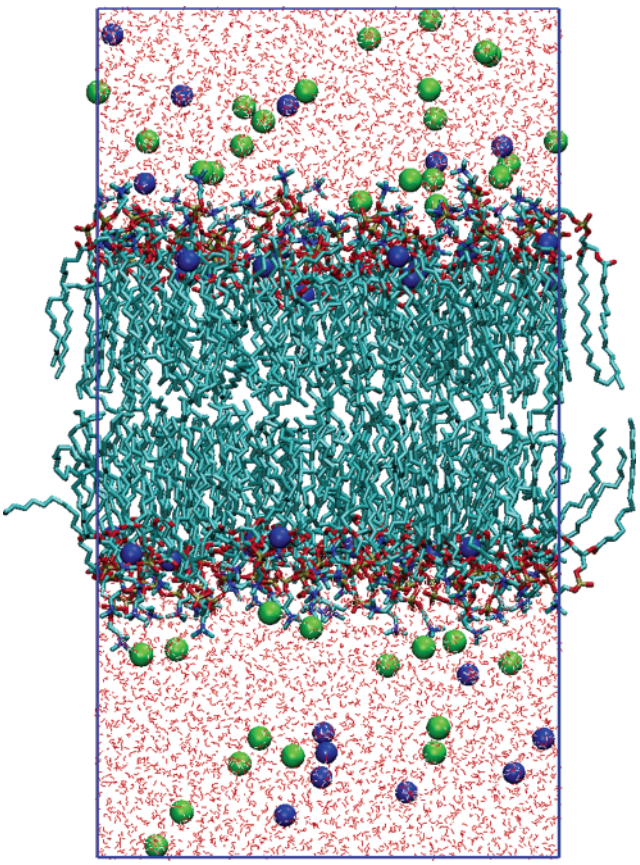

Figure 5. Snapshot from the simulation of a DPPC bilayer in an NaCl electrolyte solution. In the bathing aqueous solution, Na^+ ions are shown as blue spheres and Cl^- ions are shown as green spheres.

Bockmann et al.[96] studied the effect of NaCl salt on POPC membranes. Their simulations were performed over relatively long times of ~100 ns. They also observed that the area per lipid headgroup was diminished to a greater extent when the concentration of salt was increased. The simulations revealed a tight binding of Na^+ ions to carbonyl oxygens and the creation of complexes containing Na^+ ions and three lipids. While the Na^+ ions penetrated deeply into the bilayer and coordinated with carbonyl oxygens, Cl^- ions remained in the water phase.

Sachs et al. also studied the effect of NaCl salt on the POPC bilayers. Their simulation runs were 5 ns long. They also observed an ion double layer with Na^+ ions penetrating more toward the interior of the membrane. The ion distributions did not show any clear peaks, indicating that no strong, site-specific ion bindings existed in the system. This is contrary to the observations related to Na^+ ions made by Pandit et al. and Bockmann et al. The separation between peaks in the Na^+ and Cl^- density plots from the simulations of Sachs et al. was smaller than that observed in the simulations of Pandit et al. and Bockmann et al. Sachs et al. also studied the permeation of larger anions compared to Cl^- and observed that these permeated deeper into the membrane than did either Cl^- and Na^+ ions. This is consistent with the prediction given by the Hofmeister series. Sachs et al. studied the changes in the headgroup tilt when the headgroups interacted with the ions. They observed that Na^+ ions pushed the headgroups down toward the plane of the bilayer, while Cl^- ions pushed the headgroups in the opposite direction. Large anions had the same effect as Na^+ ions. The ability of large anions to penetrate deeper into the membrane was explained as due to their ability to dehydrate more effectively.

It may seem that the strong adsorption of Na^+ cations and a very weak adsorption of Cl^- anions by a neutral DPPC bilayer observed in the simulation of Pandit et al. contradict the electrophoretic measurements which indicate that multilamellar vesicles are not charged in the presence of monovalent salt.[89] Is it possible that a longer than 5 ns simulation will result in a stronger adsorption of Cl^- ions? This is very doubtful, since a longer 100 ns simulation by Bockmann et al. performed on a very similar system showed the same qualitative result when it came to adsorption of ions. Even longer simulations by Bockmann and Grubmuller[97] did not change the conclusion about the ionic adsorption. Simulations by Sachs et al. did not show such a dramatic difference in adsorption pattern of ions, but the simulations were only 5 ns long and were performed with a constant area per headgroup constraint, which may strongly influence the ion distribution. How then can one reconcile the conclusions of the simulations from Bockmann et al. and Pandit et al. with the electrophoretic measurements? The data from the electrophoretic measurements are based on models that introduce notions of a hydrodynamic plane and assumptions that this plane is only 0.2 nm away from the surface of the bilayer. If one assumes that the hydrodynamic entity in the electrophoretic experiment includes two to three layers of interfacial water where most of the chloride ions are concentrated, one can reconcile experiment and simulation.

Among all cations interacting with membranes, a very prominent role is played by the divalent Ca^{2+} ions. Calcium ions are an integral part of neural signal transduction.[98] They

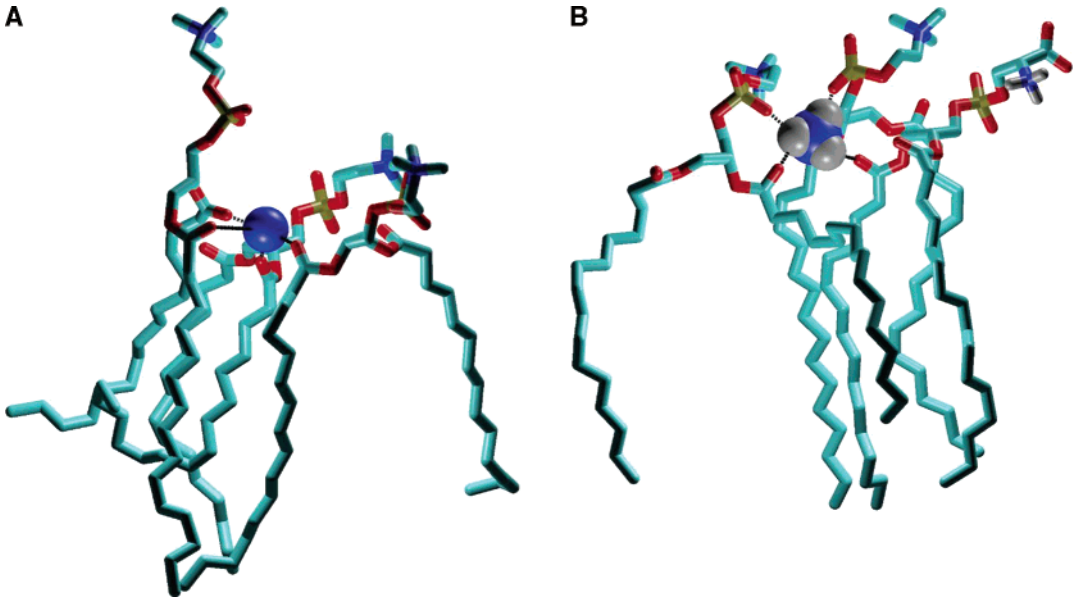

Figure 6. Snapshots of **(**A**)** Na^+ and **(**B**)** NH_4^+ ions' complexation with lipids in a simulated DPPC/DPPS mixed bilayer system with NaCl electrolyte and NH_4^+ counterions.

also trigger membrane fusion.[99] Bockmann and Grubmuller[97] performed a 200 ns simulation of a POPC bilayer in the presence of $CaCl_2$ salt to study Ca^{2+} binding to the membrane. They observed that binding of the calcium ions to the lipid carbonyl oxygens occurs in a sequential fashion. Binding of the first oxygen to the ion required 30−40 ns at a calcium concentration of 0.089 M. After 200 ns of simulation, half of the calcium ions present in the system were coordinated by four POPC molecules. Bockmann and Grubmuller also extended the previous simulation of POPC in the presence of NaCl salt to a 200 ns run. The results from a 200 ns simulation did not show much difference between this and their previous 100 ns simulation. Monoexponential fits to the curves displaying the number of coordinating water oxygens and lipid carbonyl oxygens as a function of the simulation time showed that binding times were 23 ns for Na^+ and 86 ns for Ca^{2+} ions. The work of Bockmann and Grubmuller demonstrated that simulation runs of a few hundreds of nanoseconds are required to get quantitative information about systems containing ionic species. Nevertheless, shorter runs may provide us with qualitative information about the location of ions and the general structure of the bilayer. Simulations of systems with saturated phospholipids may require shorter runs than simulations of systems with unsaturated phospholipids.

5.6. Specific Interactions of Ions with Membranes Containing a Mixture of Lipid Species

Biomembranes are complex entities that contain mixtures of lipids, sterols, and proteins. The majority of the lipids in natural membranes are either neutral or negatively charged. Very recently, a series of simulations appeared where mixtures containing neutral and charged phospholipid molecules were simulated in the presence of salt and counterions. Pandit et al.[100] simulated a mixture of DPPC/DPPS at a 5:1 ratio to probe the interactions between the lipids and the role of ions in the possible complexation of lipids. They also investigated the electrostatics of the system. Two simulations were performed, both containing the lipid mixture, NH_4^+ counterions, and NaCl salt. The simulations differed by the amount of salt: the first simulation was performed with a salt concentration of 0.19 M, and the second with 0.3 M. The trajectories were run for 15 and 20 ns, respectively. Comparison of the results from the simulations of the mixture and of the pure DPPC showed that the presence of the mixture and the addition of salt increased the propensity of DPPC to form complexes. This increased propensity was triggered by the conformational changes in the headgroups of lipids due to the presence of ions that formed bridges with the lipids. Some of the complexes with both Na^+ and NH_4^+ cations are shown in Figure 6. Cl^- anions were not observed to be involved in the bridging events. The calculated electrostatic potential again was dominated by the water dipolar contribution at the interface. It looked very similar to the potential of the pure DPPC/water system, although it displayed a small negative dip at distances larger than 1.0 nm from the surface due to the surface potential contribution.

Very recently, Murzin et al.[101] studied a bilayer containing a mixture of palmitoyloleoylphosphatidylethanolamine (POPE) and palmitoyloleoylphosphatidylglycerol (POPG) lipids in the ratio 3:1 in the presence of Na^+ counterions. The simulation was performed for 25 ns. Murzin et al. observed that Na^+ ions interacted preferentially with the PG lipids, although these interactions were not so numerous since they involved only 15% of all PGs. They also observed that Na^+ ions binded to carbonyl oxygens. Ion bridges in the PE/PG mixture were rare due to their competition with stronger direct and water mediated interlipid interactions in the bilayer.

While natural membranes contain acidic lipids and, therefore, are negatively charged, there is a need to study membranes containing cationic lipids since liposomes containing cationic lipids may be used for gene delivery.[102] Gurtovenko et al.[103] performed simulations on systems where the bilayer contained a mixture of neutral DMPC lipids and positively charged dimyristoyltrimethylammonium propane (DMTAP) lipid molecules. The bathing aqueous solution contained Cl^- anions. Eleven simulations, each at a different ratio of lipids (including the pure DMPC and pure DMTAP cases) and each of a ∼20 ns time period, were performed. It was observed that as the mole fraction of TAP increased, the orientation of water changed. The average direction of

water dipoles became inverted when the fraction of TAP molecules was larger than 50%. As a result, the dipole potential changed and increased from the value of ~600 mV for pure DMPC to ~1.2 V for pure DMTAP. Gurtovenko et al. observed that Cl^- ions were attracted to positively charged TAP headgroups but were not able to penetrate the outer boundary of the bilayer formed by the DMPC headgroups. This observation is consistent with the results from other simulations on pure PC lipids in the presence of salt.

6. Conclusions

During the past decade, computational power has increased dramatically. Now one can routinely perform simulations on bilayers for tens or hundreds of nanoseconds. This represents an increase of 3 orders of magnitude in the time length of the typical molecular dynamics run when compared to the cases of the early days of lipid simulations. The size of the simulated patch has also increased, but only slightly. Most simulations are performed on membrane patches that contain around 100 lipids per monolayer.

The advances in computational hardware and software allowed us to obtain valuable insights into the properties of aqueous solutions at the interface of phospholipid membranes. First of all, we learned that the interface between water and lipid bilayers is very broad. This was already observed in the earlier simulations.[27] Water molecules permeate lipid headgroups and reach carbonyl oxygen atoms. The influence of the bilayer on water is somewhat short ranged. It propagates to distances of ~1 nm. The layer of water next to the headgroups, the hydration layer, is strongly perturbed. It is responsible for the portion of the hydration force that is due to water. Water molecules in the hydration layer also participate in the complexation events by serving as bridging molecules in hydrogen bonded complexes between lipid molecules or lipid and sterol molecules.[104] The orientational properties of water molecules can be used to classify them, but a properly deconvoluted density may also be constructed and used for classification of interfacial water. The orientational preference of interfacial waters is displayed in the dipole potential. The sign of the dipole potential is determined by the amount of water. When the bilayer is fully hydrated, water overcompensates the dipolar contribution of the lipid headgroups. Continuum treatment of water predicts the incorrect sign of the electrostatic potential near the membrane surface.

When ions are added to water, simulations show that ion specific effects take place at the interface. Even in the presence of monovalent ions, important structural changes occur in the bilayer: the orientational properties of the headgroups are changed, the area per headgroup decreases, and ions participate in complexation between lipids. The degree of specificity depends on the ion, and experiments show that ions follow the rules predicted by the Hofmeister series. The full nature of the Hofmeister series is still not clear.

Computer simulations provide us with a useful detailed molecular description of the events, but to be sure that this is reliable, we need to compare the results from the simulations with experiments. When such a comparison is made, one should understand that the experimental results may also depend on the assumptions and models that are invoked for the experimental data interpretation. Considering the situation with aqueous-solution/phospholipid-membrane interfaces, we observe that a number of discrepancies between simulations and experiment exist. Thus, the dipole potential for PC membranes in simulations is larger than that in experiments. A strong adsorption of Na^+ ions and a very weak adsorption of Cl^- ions to neutral phosphatidylcholine membranes are somewhat inconsistent with electrophoretic measurements. We already mentioned that some of the assumptions made in the models used for the interpretation of the experiment might need to be revised. There is also a serious possibility that the potential functions, also known as the force field, that we use in the simulations are not adequate for an accurate quantitative description. The most serious deficiency of the force field may be related to the absence of charge fluctuations due to electronic polarizability. The inclusion of electronic polarizability may play an especially important role when we consider the specific behavior of the ions at the interfaces. Perera and Berkowitz[105−107] demonstrated that inclusion of polarizability into the force field changes the location of anions, such as Cl^-, Br^-, and I^-, in water clusters. Inclusion of polarizability promotes the tendency of the ion to move to the surface of the cluster. Jungwirth and Tobias[108,109] studied the distribution of salt in water slabs and observed that when polarizability is included in the force field, the ion density is increased at the interface. It is possible that inclusion of polarizability terms into simulations dealing with the aqueous-solution/phospholipid-membrane interface will result in a changed distribution of ions This may apply most especially to anions in their stronger adsorption to membrane surfaces. We are not aware of any simulations on systems containing phospholipid membranes that use polarizable force fields. Such simulations would be computationally demanding. Nevertheless, simulations that included polarizability of atoms in protein molecules have already appeared.[110]

In this review we described recent computational work that studied properties of water next to model biomembrane surfaces; we remind the reader that recent experimental work on this subject was reviewed in detail by Milhaud.[12] Structural and dynamical properties of water next to biomembranes are similar to properties of water next to other biologically important macromolecules such as DNA and proteins, and a very large amount of both experimental and computational work was done to study water at these surfaces, especially recently. Readers who are interested in this subject are advised to consult the special issue of the *Philosophical Transactions of the Royal Society of London, Series B*.[111]

Membrane processes occur on a number of different time scales. While the role of aqueous solutions in the events that take place over hundreds of nanoseconds can currently be studied using detailed simulations, other processes that take place over longer time scales require a more coarse-grained description. In some cases, it is possible to coarse grain the force field and study such phenomena as membrane elasticity or mixing and demixing of lipids using force fields that exclude water altogether.[112,113] In other cases, when the detailed description of the aqueous solution is required by the problem and the process occurs over a long time scale, multiscale methods or other special methods should be used. This is a task for future work.

7. Acknowledgments

This work was supported by the National Science Foundation under Grant No. MCB0315502.

8. References

(1) White, S. H.; Wiener, M. C. In *Permeability and Stability of Lipid Bilayers*; Disalvo, E. A., S. A. S., Eds.; CRC Press: Boca Raton, FL, 1995.

(2) Nagle, J. F.; Tristram-Nagle, S. *Biochim. Biophys. Acta* **2000**, *1469*, 159−195.

(3) Fitter, J.; Lechner, R. E.; Dencher, N. A. *J. Phys. Chem. B* **1999**, *103*, 8036−8050.

(4) Bechinger, B.; Seelig, J. *Chem. Phys. Lipids* **1991**, *58*, 1−5.

(5) Huster, D.; Jin, A. J.; Arnold, K.; Gawrisch, K. *Biophys. J.* **1997**, *73*, 855−864.

(6) Westlund, P. O. *J. Phys. Chem. B* **2000**, *104*, 6059−6064.

(7) Mendelsohn, R.; Senak, L. In *Biomolecular Spectroscopy*; Clark, J. R., Heister, R. E., Eds.; Wiley: New York, 1993.

(8) Sykora, J.; Kapusta, P.; Fidler, V.; Hof, M. *Langmuir* **2002**, *18*, 571−574.

(9) Rand, R. P.; Parsegian, V. A. *Biochim. Biophys. Acta* **1989**, *988*, 351−376.

(10) Markova, N.; Sparr, E.; Wadso, L.; Wennerstrom, H. *J. Phys. Chem. B* **2000**, *104*, 8053−8060.

(11) Binder, H.; Kohlstrunk, B.; Heerklotz, H. H. *J. Colloid Interface Sci.* **1999**, *220*, 235−249.

(12) Milhaud, J. *Biochim. Biophys. Acta* **2004**, *1663*, 19−51.

(13) Pastor, R. W. *Curr. Opin. Struct. Biol.* **1994**, *4*, 486-492.

(14) Zhou, F.; Schulten, K. *J. Phys. Chem.* **1995**, *99*, 2194−2207.

(15) Marrink, S. J.; Tieleman, D. P.; vanBuuren, A. R.; Berendsen, H. J. C. *Faraday Discuss.* **1996**, 191−201.

(16) Jakobsson, E. *Trends Biochem. Sci.* **1997**, *22*, 339−344.

(17) Tieleman, D. P.; Marrink, S. J.; Berendsen, H. J. C. *Biochim. Biophys. Acta* **1997**, *1331*, 235−270.

(18) Tobias, D. J.; Tu, K. C.; Klein, M. L. *Curr. Opin. Colloid Interface Sci.* **1997**, *2*, 15−26.

(19) Feller, S. E. *Curr. Opin. Colloid Interface Sci.* **2000**, *5*, 217−223.

(20) Forrest, L. R.; Sansom, M. S. P. *Curr. Opin. Struct. Biol.* **2000**, *10*, 174−181.

(21) Saiz, L.; Bandyopadhyay, S.; Klein, M. L. *Biosci. Rep.* **2002**, *22*, 151−173.

(22) Scott, H. L. *Curr. Opin. Struct. Biol.* **2002**, *12*, 495−502.

(23) Pratt, L. R.; Pohorille, A. *Chem. Rev.* **2002**, *102*, 2671−2691.

(24) Egberts, E.; Berendsen, H. J. C. *J. Chem. Phys.* **1988**, *89*, 3718−3732.

(25) Berkowitz, M. L.; Raghavan, K. *Langmuir* **1991**, *7*, 1042−1044.

(26) Raghavan, K.; Reddy, M. R.; Berkowitz, M. L. *Langmuir* **1992**, *8*, 233−240.

(27) Marrink, S. J.; Berkowitz, M.; Berendsen, H. J. C. *Langmuir* **1993**, *9*, 3122−3131.

(28) Alper, H. E.; Bassolinoklimas, D.; Stouch, T. R. *J. Chem. Phys.* **1993**, *99*, 5547−5559.

(29) Damodaran, K. V.; Merz, K. M. *Langmuir* **1993**, *9*, 1179−1183.

(30) Israelachvili, J. N.; Wennerstrom, H. *Langmuir* **1990**, *6*, 873−876.

(31) Schiby, D.; Ruckenstein, E. *Chem. Phys. Lett.* **1983**, *95*, 435−438.

(32) Kornyshev, A. A.; Leikin, S. *Phys. Rev. A* **1989**, *40*, 6431−6437.

(33) Leikin, S.; Kornyshev, A. A. *J. Chem. Phys.* **1990**, *92*, 6890−6898.

(34) Attard, P.; Patey, G. N. *Phys. Rev. A* **1991**, *43*, 2953−2962.

(35) Cevc, G. *J. Chem. Soc., Faraday Trans.* **1991**, *87*, 2733−2739.

(36) Leikin, S.; Kornyshev, A. A. *Phys. Rev. A* **1991**, *44*, 1156−1168.

(37) Parsegian, V. A.; Rand, R. P. *Langmuir* **1991**, *7*, 1299−1301.

(38) Leikin, S.; Parsegian, V. A.; Rau, D. C.; Rand, R. P. *Annu. Rev. Phys. Chem.* **1993**, *44*, 369−395.

(39) Kirchner, S.; Cevc, G. *J. Chem. Soc., Faraday Trans.* **1994**, *90*, 1941−1951.

(40) Leckband, D.; Israelachvili, J. *Q. Rev. Biophys.* **2001**, *34*, 105−267.

(41) Manciu, M.; Ruckenstein, E. *Langmuir* **2001**, *17*, 7582−7592.

(42) McIntosh, T. J.; Simon, S. A. *Annu. Rev. Biophys. Biomol. Struct.* **1994**, *23*, 27−51.

(43) Essmann, U.; Perera, L.; Berkowitz, M. L. *Langmuir* **1995**, *11*, 4519−4531.

(44) Aman, K.; Lindahl, E.; Edholm, O.; Hakansson, P.; Westlund, P. O. *Biophys. J.* **2003**, *84*, 102−115.

(45) Jedlovszky, P.; Mezei, M. *J. Phys. Chem. B* **2001**, *105*, 3614−3623.

(46) Israelachvili, J. *Acc. Chem. Res.* **1987**, *20*, 415−421.

(47) Ashbaugh, H. S.; Pratt, L. R.; Paulaitis, M. E.; Clohecy, J.; Beck, T. L. *J. Am. Chem. Soc.* **2005**, *127*, 2808−2809.

(48) Pandit, S. A.; Bostick, D.; Berkowitz, M. L. *J. Chem. Phys.* **2003**, *119*, 2199−2205.

(49) Ruocco, M. J.; Shipley, G. G. *Biochim. Biophys. Acta* **1982**, *691*, 309−320.

(50) Tate, M. W.; Eikenberry, E. F.; Turner, D. C.; Shyamsunder, E.; Gruner, S. M. *Chem. Phys. Lipids* **1991**, *57*, 147−164.

(51) Casal, H. L.; Martin, A.; Mantsch, H. H.; Paltauf, F.; Hauser, H. *Biochemistry* **1987**, *26*, 7395−7401.

(52) Hubner, W.; Blume, A. *Chem. Phys. Lipids* **1998**, *96*, 99−123.

(53) Pasenkiewicz-Gierula, M.; Takaoka, Y.; Miyagawa, H.; Kitamura, K.; Kusumi, A. *J. Phys. Chem. A* **1997**, *101*, 3677−3691.

(54) Pasenkiewicz-Gierula, M.; Takaoka, Y.; Miyagawa, H.; Kitamura, K.; Kusumi, A. *Biophys. J.* **1999**, *76*, 1228−1240.

(55) Lopez, C. F.; Nielsen, S. O.; Klein, M. L.; Moore, P. B. *J. Phys. Chem. B* **2004**, *108*, 6603−6610.

(56) Luzar, A.; Chandler, D. *Nature* **1996**, *379*, 55−57.

(57) Luzar, A.; Chandler, D. *Phys. Rev. Lett.* **1996**, *76*, 928−931.

(58) Clarke, R. J. *Adv. Colloid Interface Sci.* **2001**, *89*, 263−281.

(59) Liberman, Y. A.; Topaly, V. P. *Biofizika* **1969**, *14*, 452.

(60) Clarke, R. J.; Lupfert, C. *Biophys. J.* **1999**, *76*, 2614−2624.

(61) Clarke, R. J.; Kane, D.-. *Biochim. Biophys. Acta* **1997**, *1323*, 223−239.

(62) Becucci, L.; Moncelli, M. R.; Herrero, R.; Guidelli, R. *Langmuir* **2000**, *16*, 7694−7700.

(63) Brockman, H. *Chem. Phys. Lipids* **1994**, *73*, 57−79.

(64) Simon, S. A.; McIntosh, T. J.; Magid, A. D. *J. Colloid Interface Sci.* **1988**, *126*, 74−83.

(65) Smondyrev, A. M.; Berkowitz, M. L. *J. Comput. Chem.* **1999**, *20*, 531−545.

(66) Feller, S. E.; Pastor, R. W.; Rojnuckarin, A.; Bogusz, S.; Brooks, B. R. *J. Phys. Chem.* **1996**, *100*, 17011−17020.

(67) Essmann, U.; Berkowitz, M. L. *Biophys. J.* **1999**, *76*, 2081−2089.

(68) Saiz, L.; Klein, M. L. *J. Chem. Phys.* **2002**, *116*, 3052−3057.

(69) Berger, O.; Edholm, O.; Jahnig, F. *Biophys. J.* **1997**, *72*, 2002−2013.

(70) Gawrisch, K.; Ruston, D.; Zimmerberg, J.; Parsegian, V. A.; Rand, R. P.; Fuller, N. *Biophys. J.* **1992**, *61*, 1213−1223.

(71) Mashl, R. J.; Scott, H. L.; Subramaniam, S.; Jakobsson, E. *Biophys. J.* **2001**, *81*, 3005−3015.

(72) McLaughlin, S. *Annu. Rev. Biophys. Biophys. Chem.* **1989**, *18*, 113−136.

(73) Cevc, G. *Biochim. Biophys. Acta* **1990**, *1031*, 311−382.

(74) BenTal, N.; Honig, B.; Miller, C.; McLaughlin, S. *Biophys. J.* **1997**, *73*, 1717−1727.

(75) Langner, M.; Kubica, K. *Chem. Phys. Lipids* **1999**, *101*, 3−35.

(76) Hofmeister, F. *Arch. Exp. Pathol. Pharmakol.* **1888**, *24*, 247−260.

(77) Collins, K. D.; Washabaugh, M. W. *Q. Rev. Biophys.* **1985**, *18*, 323−422.

(78) Bostrom, M.; Williams, D. R. M.; Ninham, B. W. *Langmuir* **2002**, *18*, 8609−8615.

(79) Hribar, B.; Southall, N. T.; Vlachy, V.; Dill, K. A. *J. Am. Chem. Soc.* **2002**, *124*, 12302−12311.

(80) Bostrom, M.; Williams, D. R. M.; Stewart, P. R.; Ninham, B. W. *Phys. Rev. E* **2003**, *68*.

(81) Bostrom, M.; Williams, D. R. M.; Ninham, B. W. *Biophys. J.* **2003**, *85*, 686−694.

(82) Gurau, M. C.; Lim, S. M.; Castellana, E. T.; Albertorio, F.; Kataoka, S.; Cremer, P. S. *J. Am. Chem. Soc.* **2004**, *126*, 10522−10523.

(83) Netz, R. R. *Eur. Phys. J. E* **2001**, *5*, 557−574.

(84) Moreira, A. G.; Netz, R. R. *Phys. Rev. Lett.* **2001**, 8707.

(85) Moreira, A. G.; Netz, R. R. *Europhys. Lett.* **2000**, *52*, 705−711.

(86) Petrache, H. I.; Tristram-Nagle, S.; Gawrisch, K.; Harries, D.; Parsegian, V. A.; Nagle, J. F. *Biophys. J.* **2004**, *86*, 1574−1586.

(87) Pandit, S. A.; Berkowitz, M. L. *Biophys. J.* **2002**, *82*, 1818−1827.

(88) Lin, J. H.; Baker, N. A.; McCammon, J. A. *Biophys. J.* **2002**, *83*, 1374−1379.

(89) Eisenberg, M.; Gresalfi, T.; Riccio, T.; McLaughlin, S. *Biochemistry* **1979**, *18*, 5213−5223.

(90) Tatulian, S. A. *Biochim. Biophys. Acta* **1983**, *736*, 189−195.

(91) Macdonald, P. M.; Seelig, J. *Biochemistry* **1988**, *27*, 6769−6775.

(92) Akutsu, H.; Seelig, J. *Biochemistry* **1981**, *20*, 7366−7373.

(93) Binder, H.; Zschornig, O. *Chem. Phys. Lipids* **2002**, *115*, 39−61.

(94) Mukhopadhyay, P.; Monticelli, L.; Tieleman, D. P. *Biophys. J.* **2004**, *86*, 1601−1609.

(95) Pandit, S. A.; Bostick, D.; Berkowitz, M. L. *Biophys. J.* **2003**, *84*, 3743−3750.

(96) Bockmann, R. A.; Hac, A.; Heimburg, T.; Grubmuller, H. *Biophys. J.* **2003**, *85*, 1647−1655.

(97) Bockmann, R. A.; Grubmuller, H. *Angew. Chem., Int. Ed.* **2004**, *43*, 1021−1024.

(98) Alberts, B.; Johnson, A.; Lewis, J.; Raff, M.; Roberts, K.; Walter, P. *Molecular Biology of the Cell*; Garland Science: New York, 2002.

(99) Szule, J. A.; Jarvis, S. E.; Hibbert, J. E.; Spafford, J. D.; Braun, J. E. A.; Zamponni, G. W.; Wessel, G. M.; Coorssen, J. R. *J. Biol. Chem.* **2003**, *278*, 24251−24254.
(100) Pandit, S. A.; Bostick, D.; Berkowitz, M. L. *Biophys. J.* **2003**, *85*, 3120−3131.
(101) Murzyn, K.; Rog, T.; Pasenkiewicz-Gierula, M. *Biophys. J.* **2005**, *88*, 1091−1103.
(102) Mahato, R. I. *Adv. Drug Delivery Rev.* **2005**, *57*, 699−712.
(103) Gurtovenko, A. A.; Patra, M.; Karttunen, M.; Vattulainen, I. *Biophys. J.* **2004**, *86*, 3461−3472.
(104) Smondyrev, A. M.; Berkowitz, M. L. *Biophys. J.* **1999**, *77*, 2075−2089.
(105) Perera, L.; Berkowitz, M. L. *J. Chem. Phys.* **1991**, *95*, 1954−1963.
(106) Perera, L.; Berkowitz, M. L. *J. Chem. Phys.* **1992**, *96*, 8288−8294.
(107) Perera, L.; Berkowitz, M. L. *J. Chem. Phys.* **1993**, *99*, 4236−4237.
(108) Jungwirth, P.; Tobias, D. J. *J. Phys. Chem. B* **2002**, *106*, 6361−6373.
(109) Vrbka, L.; Mucha, M.; Minofar, B.; Jungwirth, P.; Brown, E. C.; Tobias, D. J. *Curr. Opin. Colloid Interface Sci.* **2004**, *9*, 67−73.
(110) Harder, E.; Kim, B.; Friesner, R. A.; Berne, B. J. *J. Chem. Theory Comput.* **2005**, *1*, 169−180.
(111) Daniel, R. M.; Finney, J. L.; Stoneham, L. *Philos. Trans. R. Soc. London, Ser. B* **2004**, *359*, 1141−1328.
(112) Farago, O. *J. Chem. Phys.* **2003**, *119*, 596−605.
(113) Brannigan, G.; Brown, F. L. H. *J. Chem. Phys.* **2004**, *120*, 1059−1071.

CR0403638